Bridged polysilsesquioxane films *via* photoinduced sol–gel chemistry†

Abraham Chemtob,[a] Cindy Belon,[a] Céline Croutxé-Barghorn,*[a] Jocelyne Brendlé,[b] Michel Soulard,[b] Séverinne Rigolet,[b] Vincent Le Houérou[c] and Christian Gauthier[c]

Received (in Montpellier, France) 16th December 2009, Accepted 10th March 2010
First published as an Advance Article on the web 24th March 2010
DOI: 10.1039/b9nj00763f

The synthesis and characterization of bridged polysilsesquioxane films was performed *via* a photoacid-catalyzed sol–gel method using a series of three precursors with different organic moiety structures.

Organo-bridged trialkoxysilane precursors $[(R'O)_3Si–R–Si(OR')_3]$ were extensively implemented in the 1990s for the synthesis of numerous organosilica xerogels and aerogels, often referred to as bridged polysilsesquioxanes, through conventional sol–gel processing.[1,2] The versatility of the organic moiety R, combined with sol–gel process adaptability (catalyst, solvent, temperature, *etc.*), enabled tailoring of the textural, physical and chemical properties of the resulting nanocomposite solids. Another peculiar property of these bridged precursors is their ability to self-organize with short-range and occasionally long-range periodicity,[3,4] depending on the organic unit and the experimental conditions. However, despite many desirable characteristics of the resultant hybrids, their synthesis has mostly relied on a classical hydrolytic sol–gel route in solution so as to form gels. An alternative methodology was reported notably by Corriu *et al.*, who performed solid state hydrolysis/condensations without solvent in order to induce the formation of highly ordered organosilica films.[5,6] In addition, Loy *et al.* have reported an anhydrous sol–gel polymerization in supercritical carbon dioxide to prepare a phenylene-bridged polysilsesquioxane.[7]

Here, we report a rather different strategy to synthesize bridged organosilica films through a photoinduced sol–gel process of a bis-silylated precursor. A variation of this methodology was first described in 2005 by Kowalewska using various onium salt-based photoinitiators.[8] However, only one type of bridged precursor was studied, without examining the textural and mechanical characterizations of the films, as well as their possible self-organization. Brinker *et al.* also reported in 2002 the use of light exposure with bridged silsesquioxanes, not for photoacid catalysis of the sol–gel process, but the photoisomerization of an azobenzene moiety included within the organic bridged fragment.[9] Since the pioneering work of Crivello, iodonium and sulfonium salts have been widely used as photoacid generators, mainly for cationic photopolymerization.[10] Upon irradiation by UV light, Brønsted acids (or photoacids) of the structure H^+X^-, based on non-nucleophilic anions X^-, are readily generated to initiate the cationic polymerization of multifunctional monomers or oligomers of mainly the epoxy or vinyl ether type. Very few studies have addressed the concept of a photoacid-catalyzed sol–gel process for alkoxysilanes (photo sol–gel).[11] In 1978, Fox *et al.* first proved that onium salt photolysis was efficient at promoting the hydrolysis–polycondensation of alkoxysilyl precursors without any solvent.[12]

In this study, we have chosen three bridged precursors with different organic moiety structures (Scheme 1). Besides the linear rod *p*-arylene precursor **1**, we have considered a more flexible molecule presenting an octane aliphatic chain, **2**. The case of an amino functional derivative, **3**, was also investigated. The synthesis of bridged polysilsesquioxane films was performed by following a photoacid-catalyzed sol–gel method in the presence of a commercial diaryl iodonium salt (Irgacure 250). As the superacid HPF_6 is liberated *in situ via* onium salt photolysis, the photolatent formulation, comprising only the molecular bis-silylated precursor and a cationic photoinitiator (PI, 2% wt), can be handled without solvent. Another key feature in a photo sol–gel process concerns the hydrolysis step, ensured by the simple diffusion of moist air within the liquid film. This avoids any addition of water and consequently the problem of rapid gelation, which is a characteristic trait of the bridged precursors. The sol–gel reaction is then triggered by simple UV exposure of the liquid film, circumventing the formation of a sol and its further transformation into a gel. As shown in Scheme 2, the solids obtained by this innovative photochemical route (**F1–F3**) were systematically compared with xerogels prepared by a traditional HCl-catalyzed sol–gel process (**X1–X3**), in regard to the reaction kinetics, as well as their chemical and textural properties. Finally, attempts were made to characterize the mechanical properties of the films and to evidence whether this new solvent-free route might be of interest for increasing the level of ordering in the hybrid material.

For all precursors, dry and insoluble films (**F1–F3**) were obtained with a photo sol–gel process after an exposure time of 1.15 s under a UV conveyor (H lamp). As shown in Table 1, the efficiency of the photo sol–gel process was confirmed by

[a] *Département de Photochimie Générale, CNRS, ENSCMu, University of Haute-Alsace, 3 rue Alfred Werner, 68093 Mulhouse Cedex, France. E-mail: Celine.Croutxe-Barghorn@uha.fr; Fax: +33 (0)3 89 33 50 14; Tel: +33 (0)3 89 33 50 17*
[b] *Equipe Matériaux à Porosité Contrôlée, IS2M, CNRS, LRC 7228, University of Haute-Alsace, 3 rue Alfred Werner, 68093 Mulhouse Cedex, France*
[c] *Institut Charles Sadron, CNRS, UPR 22, University of Strasbourg, 23 rue du Loess, BP 84047, 67034 Strasbourg Cedex 2, France*

† Electronic supplementary information (ESI) available: CP-MAS ^{29}Si NMR spectra of the photocured films **F1–F3** (Fig. S1). CP-MAS ^{13}C NMR spectra of the photocured films **F1–F3** (Fig. S2). *In situ* photographs of the moving tip during a scratch experiment for **F1** and **F3** films when applying an increasing normal load (Fig. S3). See DOI: 10.1039/b9nj00763f

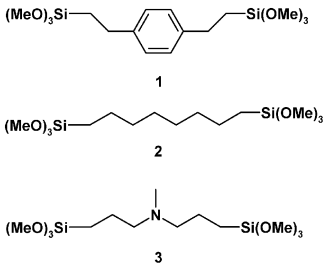

Scheme 1 The structures of the bridged precursors.

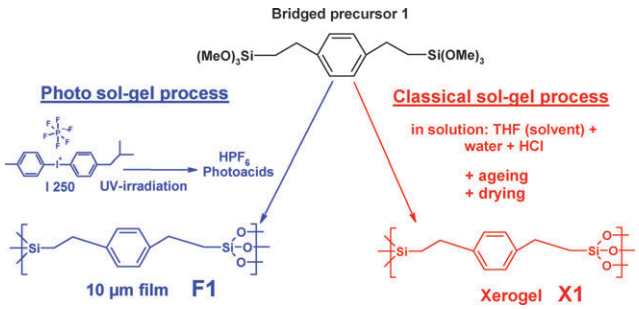

Scheme 2 The two routes towards bridged polysilsesquioxanes that were investigated in parallel: the photoacid-catalyzed sol–gel process (**F1**) and a traditional HCl-catalyzed sol–gel process (**X1**).

^{29}Si CP MAS NMR, which showed in all cases three signals corresponding to T^1 (−49 ppm, C–*Si*$(OR)_2$(O–Si)), T^2 (−58 ppm, C–*Si*(OR)$(O–Si)_2$) and T^3 (−67 ppm, C–*Si*$(O–Si)_3$) siloxane species.† Deconvolution[13] and integration of these signals showed a moderate degree of condensation, lying between 69 and 77%. Although CP-MAS spectra are not quantitative, it was preliminarily proved that they did not reveal any significant change in peak intensity compared to single pulse experiments (provided that a suitable contact time of 3 ms was selected).[8,14,15] For all the photoacid-catalyzed films, a lower level of condensation was reached compared to that of the solids prepared by a conventional sol–gel process (in THF using HCl as the catalyst). Whatever the structure of the solid, film or xerogel, a greater degree of condensation was achieved with the more flexible organic spacer of monomers **2** or **3**, as would be expected from sol–gel chemistry.

Regarding the organic moiety, its integrity was checked by ^{13}C CP-MAS NMR.† Characteristic resonances at ∼128 and ∼144 ppm, assigned to the aromatic carbons of **F1**, were identified, while **F2** and **F3** exhibited, respectively, the expected signals at ∼30 and ∼60 ppm, assigned to CH_2–(CH_2–) and CH_2–($NCH_3(CH_2)$–). In all films, a weak peak at 50.4 ppm was detected, corresponding to residual methoxy functions, and thus confirming a non-fully condensed structure. Another interesting aspect is the significant weight loss after UV irradiation. This decrease, which was estimated to be between 22 and 28 wt% (Table 1), can be accounted for by water and methanol, the by-products of hydrolysis and condensation. These values are in agreement with the levels of condensation found for the bridged polysilsesquioxanes. The specific surface area of the solids was also determined by nitrogen adsorption experiments using the BET method. Films **F1–F3** presented no specific surface area ($S_{BET} \leq 11$ m^2 g^{-1}), as well as their corresponding xerogels.

The photoinduced sol–gel process was followed by FTIR spectroscopy. After exposure to UV irradiation, the various IR spectra were found to be consistent with the formation of a complex bridged polysilsesquioxane network. With precursor **1**, for example (Fig. 1), the Si–O–CH_3 group absorbing close to 2840 cm^{-1} (CH_3 symmetric stretch) strongly diminished after irradiation. Accordingly, the spectral region between 3000 and 3700 cm^{-1}, assigned to O–H stretching vibrations, evolved appreciably under UV irradiation, which can be attributed to the formation of hydrogen-bonded silanols (Si–OH). In accordance with hydrolysis reactions, a strong band at 900 cm^{-1}, due to the Si–O stretching vibration of silanols, arose. The asymmetric stretching band of siloxanes (Si–O–Si) at 1050 cm^{-1} also grew in a pronounced way, which is characteristic of silica network formation. FTIR was also useful, as the hydrolysis rate could be evaluated for the different precursors by following the decrease in the methoxy group (Si–O–CH_3) band close to 2840 cm^{-1} as a function of UV exposure time (Fig. 2). A slower methoxysilyl conversion was reported with **2** and **3** compared to precursor **1**. In the specific case of a photo sol–gel process, the extent of hydrolysis is mainly controlled by the ability of atmospheric water to diffuse within the film (for this reason, the relative humidity was controlled and kept constant).[11] Given the low amount of water present in the film (no water was initially added to the precursor), alkoxy hydrolysis is assumed to be a rather slow process. The greater hydrophobicity of **2** compared to **1** presumably accounts for the lower hydrolysis rate found for the aliphatic precursor. In the case of **3**, the reactivity of the Si–OMe group towards water is also affected by the basicity of the amino functions, which may possibly react with the

Table 1 Characterization of the hybrid films (**F*i***) formed *via* a photo sol–gel methodology and their analogous xerogels (**X*i***) formed through a conventional sol–gel protocol. *i* corresponds to the bridged precursor employed (**1–3**)

			Film weight loss (wt%)[a]		^{29}Si CP MAS NMR (%)				
Solvent	Catalyst	Name	After irradiation	After 48 h of post-curing	T^1	T^2	T^3	Degree of condensation (%)	S_{BET}/m^2 g^{-1}
—	HPF_6 (photoacids)	**F1**	28	28	1	91	8	69 (±5)	8
—	HPF_6 (photoacids)	**F2**	12	22	10	62	28	75 (±2)	10
—	HPF_6 (photoacids)	**F3**	15	27	7	55	38	77 (±2)	11
THF	HCl	**X1**	—	—	0	75	25	75 (±5)	< 10
THF	HCl	**X2**	—	—	1	68	31	77 (±2)	< 10
THF	HCl	**X3**	—	—	0	24	76	92 (±2)	< 10

[a] The weight loss in both cases is given with respect to the initial mass of the sample.

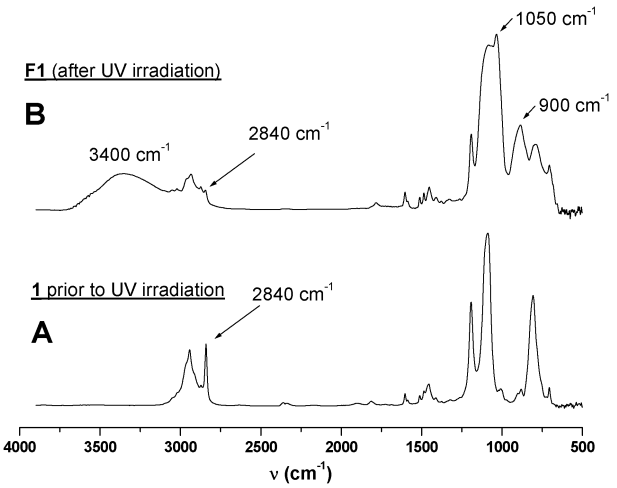

Fig. 1 An FTIR study of the photo sol–gel process of bridged precursor **1** (A) before and (B) after UV irradiation. Irradiation conditions: H-bulb lamp, 7.3 J cm^{-2}, exposure time of 1.15 s.

photoacids, as evidenced from the appearance of a growing band at 1040 cm^{-1}, attributed to the formation of NH^+ functions. The effect of the alkoxy substituent was even more striking, since substituting methoxy for ethoxy groups led to unpolymerized liquid films. Interestingly, densification occurred additionally by continued condensation reactions, even after UV irradiation, as evidenced from the weight loss (Table 1) and the data collected from the IR spectra (Fig. 2), which both indicate a progressive increase in methoxy conversion during the post-curing of the film. Thus, the hydrolysis of **F3** increased from 12 to 67% when the solid was left for 1 h in the dark at ambient temperature following UV treatment. Nevertheless, the living character of the UV curing process may be problematic for controlling the sol–gel reaction.

X-Ray diffraction (XRD) experiments were also conducted on hybrid films and xerogels to assess their respective ability to self-organize (Fig. 3). In contrast to purely inorganic silica consisting of symmetric SiO_4 tetrahedrons, the presence of a

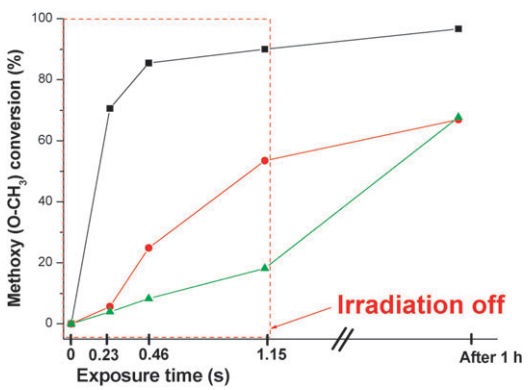

Fig. 2 The evolution of methoxy conversion (Si–O–CH_3) throughout the UV irradiation and during sample ageing (dark curing) for different bridged precursors: (■: **1**), (●, **2**) and (▲, **3**). For this, the decay of the FTIR band close to 2840 cm^{-1} (CH_3 symmetric stretch) was monitored for different exposure times under the UV conveyor (H-bulb lamp).

bridged organic group in $R(SiO_{\frac{3}{2}})_2$ materials is known to decrease the symmetry of the precursors, thereby allowing interactions between the organic moieties and promoting anisotropic organization.[16] For precursors **1** and **3**, it turned out that their diffraction patterns were essentially the same, whatever the sol–gel method implemented. No sharp Bragg signal was detected in either case, suggesting the absence of long-range crystal organization. On the other hand, two broad signals were particularly visible that clearly reflected a local organization at the nanometer scale through van der Waals interactions. The first one, centered at ~4.5 Å, which appeared in all the diagrams and the silsesquioxane materials in general, was ascribed to the contribution of the Si–O–Si distance.[17] The second diffraction, at the lowest angle, may account for the Si–R–Si distance in the organic spacer (d_p). This was confirmed by the experimental d_p values (10.3 Å for **F1** and **F3**), which fitted relatively well with the length of the organic moiety calculated by a molecular simulation (semi-empirical AM1 model) using the program Hyperchem: 10.8 and 10.5 Å for **1** and **3**, respectively. In these cases, the photoinduced process had, in turn, a moderate impact on the level of ordering. Some possible reasons are the absence of crystalline structure in the precursors themselves, or simply structure modification due to the condensation itself.[18] In addition, the reaction proceeds without solvent, but with the release of a significant amount of methanol, which may act as a co-solvent and alter the molecular interactions between organic groups that are essential for crystalline bond formation. In contrast, a marked difference in the diffraction patterns of **X2** and **F2** was evidenced from the appearance of a sharp and strong signal at 14.1 Å in this latter case. The structures of the hybrid films resulting from the photo sol–gel process showed a much higher periodicity of the organic spacer than that of its analogue prepared by a conventional sol–gel process. Although, precursor **2** is unable to develop strong hydrogen-bonding interactions, it seems that the simple van der Waals-type interactions between hydrophobic hydrocarbon chains were sufficient to induce a self-organization of the alkene units. The crystalline character of a long alkylene chain-bridged silsesquioxane has already been reported by Moreau *et al.*, who stated that a long enough chain was required to achieve high structural ordering.[19]

Finally, a first attempt was made to characterize the mechanical behaviours of the photocured films. The mechanical properties of bridged polysilsesquioxane films is a subject of great interest that has hitherto been poorly explored in comparison to thermal analysis.[2] **F1** and **F3** films were thus deposited onto a glass plate and scratch resistance tests implemented (**F2** was discarded because of poor wetting on this substrate).† For this, we measured the minimum normal loads of a moving scratching tip to first delaminate and then crack the films. Both films displayed a typical elastic behaviour, similar to that of a glass-like film, as the coatings cracked without any preliminary signs of plasticity. A low load of 1.48 N was sufficient to crack the **F1** coating; moreover, no delamination appeared before cracking. The rigid benzyl group may account for this result more than the limited level of condensation of the inorganic network. With **F3**, delamination occurred from 2.02 N, but cracks appeared only at a much

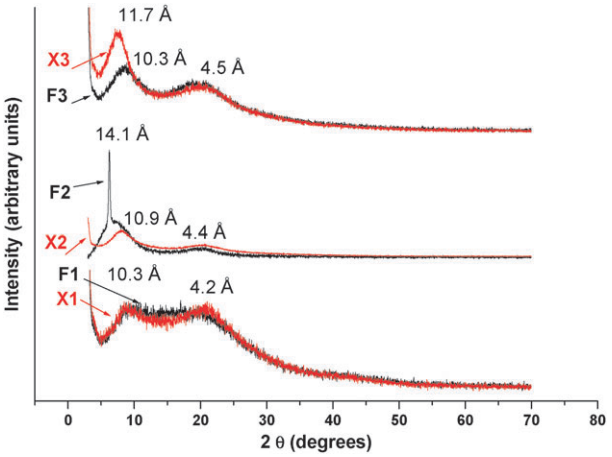

Fig. 3 X-Ray powder diffraction patterns of xerogels (**X1–X3**) and their corresponding photoinduced sol–gel films (**F1–F3**).

higher force value (5.91 N), showing the remarkable compliance and resistance of this hybrid film.

There are many indications that the photochemical sol–gel route reported in this work is advantageous for the synthesis of bridged polysilsesquioxanes. It gives access to films in a matter of seconds, whereas the majority of these hybrid materials have previously been synthesized as powders. Significant levels of condensation of the silica network (69–77%) were achieved by this methodology through catalysis by UV-generated H^+X^- superacids, thereby avoiding post-synthesis treatment. Another distinctive feature was the living character of the curing process: once the degradation of the photocatalytic onium salt had been photoinitiated, the inorganic polymerization proceeded and continued, even after terminating the UV irradiation. Finally, self-organization was evidenced for the photocured films, and even crystal-like behaviour for bridged precursor **2**.

Experimental

All manipulations were carried out in air at ambient temperature. The solvents were dried and distilled before use. The bridged precursors 1,4-bis(trimethoxysilylethyl)benzene (**1**), 1,8-bis-(trimethosilyl)octane (**2**), 1,7-bis(3-trimethoxysilylpropyl)-*N*-methylamine (**3**) and their triethoxysilyl analogues were purchased from ABCR and used without further purification. The cationic photoinitiator based on a hexafluorophosphate iodonium salt (Irgacure 250) was provided by Ciba Speciality Chemicals. Byk 333, supplied by BYK Chemie, is a surface wetting agent based on a polyether-modified polydimethyl-siloxane. For all experiments, an effective liquid film thickness of 10 μm (±2 μm) was assessed by profilometry using an Altisurf 500 workstation (Altimet) equipped with a 350 μm AltiProbe optical sensor.

To obtain ^{29}Si and ^{13}C solid state NMR spectra, cross polarization magic angle spinning (CP-MAS) experiments were performed on a Bruker Avance II 400 spectrometer with a Bruker double channel 7 mm probe. For this, zirconium rotors were employed at 79.48 and 100.6 MHz, using a recycling delay between 3 and 17 s, depending on the ^{1}H spin lattice relaxation times (t_1), estimated by an inversion recovery pulse sequence, a spinning frequency of 4 kHz and contact times of 3 and 1 ms, respectively. In both cases, chemical shifts were relative to tetramethylsilane. In ^{1}H–^{29}Si CP-MAS NMR experiments, these recording conditions (adequate contact times) ensured a semi-quantitative determination of the proportion of T^n Si substructures. For the photocured films, a scratched fragment was withdrawn, whereas a portion of the powder was taken in the case of the HCl-catalyzed xerogels. The hydrolysis kinetics (methoxy conversion) were followed using FTIR by monitoring the decrease in the area of the characteristic band close to 2840 cm^{-1} (CH_3 symmetric stretch) after several passes under the UV-conveyor. For this, samples were deposited onto a barium fluoride crystal and analyzed in transmission with a Vertex 70 (Bruker) spectro-photometer equipped with a DTGS detector with a spectral resolution of 4 cm^{-1}. Surface area measurements were conducted on a Micromeritics ASAP 2000 porosimeter using high purity nitrogen as an adsorbate at 77 K. Surface areas were determined using the BET equation. Samples were de-gassed at 120 °C for 60 h prior to measurements. X-Ray diffraction (XRD) patterns were recorded using a Philips X-pert diffractometer operating with Cu-Kα radiation (λ = 0.15418 nm) between 3 and 70° 2θ, with a step of 0.02° per 2 s. The solids were ground in an agate mortar before been pressed into a sample holder (samples **F1**, **F3**, **X1**, **X2** and **X3**) or used as films (sample **F2**). Theoretical lengths of the organic moiety were calculated using the Hyperchem molecular modelling system. The molecule structures were built and optimized using the semi-empirical molecular orbital model AM1, and the resulting Si–R–Si distances reported. The scratch resistance of the UV-cured films deposited onto glass plates was characterized at room temperature using the apparatus described in previous publications.[20,21] The tip was a 116 μm diameter diamond sphere and the sliding speed was kept constant (0.03 mm s^{-1}). Stepwise normal load ramps were performed in the range 0.025 to 6 N. At each force step, the tip moved over a distance of 1 mm in order to obtain a groove, which could be analyzed in terms of a steady state regime. Then, the size and shape of the grooves left on the coatings were analyzed, and pictures were taken with the help of an *in situ* microscope equipped with a CCD camera.†

Photo sol–gel process

To 2 g of precursor was added 40 mg of photoinitiator (2% wt) and 6 mg of Byk 333 (0.3% wt). Before UV irradiation, films were applied onto glass slides (10 × 10 cm, Brot) by means of an Elcometer 4340 motorised film applicator equipped with a spiral bar coater to apply a pre-determined film thickness. The effective liquid film thickness of 10 μm was kept constant, whatever the precursor used. Hydrolysis and polycondensation were then performed at ambient temperature with five successive passes in a UV conveyor (Qurtech) equipped with an H-bulb lamp (Fusion UV systems). The belt speed of the conveyor was set to 10 m min^{-1} and the lamp intensity to 100%. Under these conditions, the light dose received by the sample after each pass was 1.46 J cm^{-2}, which

corresponds to an exposure time of 0.23 s. The atmospheric humidity in all runs was maintained at between 34–39%.

Conventional sol–gel process

The hybrid xerogels were prepared according to the following general sol–gel procedure; their preparation is given in the case of precursor **1**. To 2 g (5.33×10^{-3} mol) of **1** in 13.34 mL of dry THF was added 0.58 g of a 1 M HCl solution (3.20×10^{-2} mol of water, 6 mol equiv.). In all experiments, 0.4 M THF solutions of the bridged precursors were employed. The homogeneous solution was stirred at room temperature for 48 h. Gels formed in most cases within several hours. After curing at room temperature for 24 h, the gel was crushed. The collected solid was washed three times with diethyl ether, filtered and dried in a vacuum (100 mBar) at 150 °C for 24 h.

References

1 R. J. P. Corriu, *Angew. Chem., Int. Ed.*, 2000, **39**, 1376–1398.
2 K. J. Shea and D. A. Loy, *Chem. Mater.*, 2001, **13**, 3306–3319.
3 S. Fujita and S. Inagaki, *Chem. Mater.*, 2008, **20**, 891–908.
4 J. J. E. Moreau, L. Vellutini, M. Wong Chi Man and C. Bied, *J. Am. Chem. Soc.*, 2001, **123**, 1509–1510.
5 B. Boury, F. Ben and R. J. P. Corriu, *Angew. Chem., Int. Ed.*, 2001, **40**, 2853–2856.
6 H. Muramatsu, R. J. P. Corriu and B. Boury, *J. Am. Chem. Soc.*, 2003, **125**, 854–855.
7 D. A. Loy, E. M. Russick, S. A. Yamanaka, B. M. Baugher and K. J. Shea, *Chem. Mater.*, 1997, **9**, 2264–2268.
8 A. Kowalewska, *J. Mater. Chem.*, 2005, **15**, 4997–5006.
9 N. Liu, K. Yu, B. Smarsly, D. R. Dunphy, Y.-B. Jiang and C. J. Brinker, *J. Am. Chem. Soc.*, 2002, **124**, 14540–14541.
10 J. V. Crivello, *J. Polym. Sci., Part A: Polym. Chem.*, 1999, **37**, 4241–4254.
11 For further references on the photoinduced sol–gel process, see: A. Chemtob, C. Belon, C. Croutxe-Barghorn and S. Rigolet, *Macromolecules*, 2008, **41**, 7390–7398.
12 F. J. Fox, R. W. Noren and G. E. Krankkala, *US Pat.* 4101513, Minnesota Mining and Manufacturing Co., USA, 1978.
13 D. Massiot, F. Fayon, M. Capron, I. King, S. Le Calve, B. Alonso, J. O. Durand, B. Bujoli, Z. Gan and G. Hoatson, *Magn. Reson. Chem.*, 2002, **40**, 70–76.
14 G. Cerveau, R. J. P. Corriu and C. Fischmeister-Lepeytre, *J. Mater. Chem.*, 1999, **9**, 1149–1154.
15 G. Cerveau, R. J. P. Corriu, C. Lepeytre and P. H. Mutin, *J. Mater. Chem.*, 1998, **8**, 2707–2713.
16 B. Boury and R. Corriu, *Chem. Rec.*, 2003, **3**, 120–132.
17 F. Lerouge, G. Cerveau and R. J. P. Corriu, *New J. Chem.*, 2006, **30**, 1364–1376.
18 P. Dieudonné, M. Wong Chi Man, B. P. Pichon, L. Vellutini, J.-L. Bantignies, C. Blanc, G. Creff, S. Finet, J.-L. Sauvajol, C. Bied and J. J. E. Moreau, *Small*, 2009, **5**, 503–510.
19 J. J. E. Moreau, L. Vellutini, P. Dieudonné, M. Wong Chi Man, J.-L. Bantignies, J.-L. Sauvajol and C. Bied, *J. Mater. Chem.*, 2005, **15**, 4943–4948.
20 C. Gauthier, S. Lafaye and R. Schirrer, *Tribol. Int.*, 2001, **34**, 469–479.
21 C. Gauthier and R. Schirrer, *J. Mater. Sci.*, 2000, **35**, 2121–2130.

